Cellular/Molecular

Distinct Actions of Voltage-Activated Ca^{2+} Channel Block on Spontaneous Release at Excitatory and Inhibitory Central Synapses

Timur Tsintsadze,[1,3]* Courtney L. Williams,[1,3]* Dennis J. Weingarten,[2] Henrique von Gersdorff,[2] and Stephen M. Smith[1,3]

[1]Division of Pulmonary and Critical Care Medicine, Department of Medicine and [2]Vollum Institute, Oregon Health and Science University, Portland, Oregon 97239, and [3]Section of Pulmonary and Critical Care Medicine, VA Portland Health Care System, Portland, Oregon 97239

At chemical synapses, voltage-activated calcium channels (VACCs) mediate Ca^{2+} influx to trigger action potential-evoked neurotransmitter release. However, the mechanisms by which Ca^{2+} regulates spontaneous transmission have not been fully determined. We have shown that VACCs are a major trigger of spontaneous release at neocortical inhibitory synapses but not at excitatory synapses, suggesting fundamental differences in spontaneous neurotransmission at GABAergic and glutamatergic synapses. Recently, VACC blockers were reported to reduce spontaneous release of glutamate and it was proposed that there was conservation of underlying mechanisms of neurotransmission at excitatory and inhibitory synapses. Furthermore, it was hypothesized that the different effects on excitatory and inhibitory synapses may have resulted from off-target actions of Cd^{2+}, a nonselective VACC blocker, or other variations in experimental conditions. Here we report that in mouse neocortical neurons, selective and nonselective VACC blockers inhibit spontaneous release at inhibitory but not at excitatory terminals, and that this pattern is observed in culture and slice preparations as well as in synapses from acute slices of the auditory brainstem. The voltage dependence of Cd^{2+} block of VACCs accounts for the apparent lower potency of Cd^{2+} on spontaneous release of GABA than on VACC current amplitudes. Our findings indicate fundamental differences in the regulation of spontaneous release at inhibitory and excitatory synapses by stochastic VACC activity that extend beyond the cortex to the brainstem.

Key words: calcium channel; mEPSC; minis; mIPSC; spontaneous; VGCC

Significance Statement

Presynaptic Ca^{2+} entry via voltage-activated calcium channels (VACCs) is the major trigger of action potential-evoked synaptic release. However, the role of VACCs in the regulation of spontaneous neurotransmitter release (in the absence of a synchronizing action potential) remains controversial. We show that spontaneous release is affected differently by VACCs at excitatory and inhibitory synapses. At inhibitory synapses, stochastic openings of VACCs trigger the majority of spontaneous release, whereas they do not affect spontaneous release at excitatory synapses. We find this pattern to be wide ranging, holding for large and small synapses in the neocortex and brainstem. These findings indicate fundamental differences of the Ca^{2+} dependence of spontaneous release at excitatory and inhibitory synapses and heterogeneity of the mechanisms of release across the CNS.

Introduction

Spontaneous release of neurotransmitter supports synapse maturation and maintenance, homeostasis, and plasticity (Jensen et al., 1999; McKinney et al., 1999; Kombian et al., 2000; Verhage et al., 2000; Sutton and Schuman, 2006). In addition to these functions, spontaneous release regulates neuronal excitability and action potential firing, indicating further physiological importance of this form of transmission (Cohen and Miles, 2000; Carter and Regehr, 2002). The recent proposal that different vesicle pools underlie spontaneous and evoked release, and that these mediate distinct functions, has emphasized the importance of precisely

Received Nov. 10, 2016; revised March 8, 2017; accepted March 13, 2017.

Author contributions: H.v.G. and S.M.S. designed research; T.T., C.L.W., and D.J.W. performed research; T.T., C.L.W., D.J.W., and S.M.S. analyzed data; T.T., C.L.W., H.v.G., and S.M.S. wrote the paper.

This work was supported by National Institute of General Medical Sciences Grant R01 GM097433 (S.M.S.); U.S. Department of Veterans Affairs Grant BX002547 (S.M.S.); NIDCD Grant DC012938 (H.v.G.); National Heart, Lung, and Blood Institute Grant T32HL083808 (C.L.W.); NINDS Grant 1F31NS083309 (C.L.W); and an international Erasmus Mundus grant from the European Union (D.J.W.).

*T.T. and C.L.W. contributed equally to this work.

Correspondence should be addressed to Stephen M. Smith, VA Portland Health Care System, 3710 Southwest U.S. Veterans Hospital Road, R&D 24, Portland, OR 97239. E-mail: smisteph@ohsu.edu.

DOI:10.1523/JNEUROSCI.3488-16.2017

 0270-6474/17/374301-10$15.00/0

understanding both forms of transmission (Autry et al., 2011; Kavalali et al., 2011).

Voltage-activated calcium channels (VACCs) are well established as key triggers of evoked synaptic transmission, but this is less clear for spontaneous release where the probability of presynaptic VACC activation is low because of the hyperpolarized resting membrane potential (Matthews and Wickelgren, 1977; Llinás et al., 1989; Wheeler et al., 1994). We determined, in cultured cortical neurons, that spontaneous release of glutamate was independent of VACCs, while spontaneous release of GABA was strongly regulated by VACCs (Vyleta and Smith, 2011; Williams et al., 2012). These surprising results indicate there are substantial differences between key mechanisms governing release at excitatory and inhibitory synapses and point to further differences between spontaneous and evoked release. In contrast, it was proposed that a substantial fraction of spontaneous release of glutamate is VACC dependent at small and large central synapses, consistent with the more conservative proposal that inhibitory and excitatory release mechanisms are similarly regulated (Ermolyuk et al., 2013; Dai et al., 2015).

In this study we have set out to readdress this fundamental question of whether VACCs regulate spontaneous release of GABA and glutamate differently at mammalian central synapses. We have extended our experiments to acute neocortical slices in addition to cell cultures, tested whether the actions of Cd^{2+} on spontaneous release can be entirely attributed to its actions as an inorganic nonselective VACC blocker, determined whether the actions on spontaneous release of organic VACC blockers are equivalent to Cd^{2+}, and examined whether VACC block affects spontaneous release at synapses in the auditory brainstem (Forsythe, 1994; von Gersdorff and Borst, 2002). Our results indicate that the regulation of miniature EPSCs (mEPSCs) by VACCs is fundamentally different from that of miniature IPSCs (mIPSCs) at both small bouton-type and large calyx-type central synapses.

Materials and Methods

Slice preparation. All animal procedures were approved by the VA Portland Health Care System (VAPORHCS) and Oregon Health and Science University Institutional Animal Care and Use Committees. Mouse pups of either sex were used to prepare acute slices from the neocortex or the medial nucleus of the trapezoid body (MNTB) at postnatal day 12 (P12)–P16 and P10–P12, respectively, as described previously (Forsythe, 1994; Borst and Sakmann, 1996; Taschenberger and von Gersdorff, 2000). Animals were anesthetized using isoflurane and decapitated. Brains were rapidly removed and placed in oxygenated ice-cold artificial CSF (ACSF). ACSF for cortical pyramidal cells had the following composition (in mM): 129 NaCl, 3.2 KCl, 1.5 $CaCl_2$, 1 $MgCl_2$, 25 $NaHCO_3$, 0.34 Na_2HPO_4, 0.44 KH_2PO_4, and 5 glucose. For neurons of the MNTB we used (in mM) 125 NaCl, 2.5 KCl, 1.5 $CaCl_2$, 1 $MgCl_2$, 25 $NaHCO_3$, 1.25 Na_2HPO_4, 2 Na-pyruvate, 3 myo-insoitol, 0.44 ascorbic acid, and 10 glucose. Slices (300 μm) were cut using Vibratome (VT 1200S; Leica) and kept in oxygenated (95% O_2 and 5% CO_2, pH 7.3) in modified ACSF. For cortical slices NaCl was substituted by choline chloride in equimolar concentration at room temperature at least 1 h before use. Individual slices were then transferred to the recording chamber where they were fully submerged and superfused with oxygenated ACSF at room temperature at a rate of 5–9 ml/min.

Neocortical culture preparation. Neocortical neurons were isolated from postnatal day 1–2 mouse pups as described previously (Phillips et al., 2008). All animal procedures were approved by the VAPORHCS Institutional Animal Care and Use Committee in accordance with the U.S. Public Health Service *Policy on Humane Care and Use of Laboratory Animals* and the National Institutes of Health *Guide for the Care and Use of Laboratory Animals*. Animals were decapitated following general anesthetic with isoflurane, and then the cerebral cortices were removed. Cortices were incubated in trypsin and DNase and then dissociated with a heat polished pipette. Dissociated cells were cultured in MEM plus 5% FBS on glass coverslips. Cytosine arabinoside (4 μM) was added 48 h after plating to limit glial division. Cells were used after a minimum of 8 d in culture for VACC current recordings or 14 d in culture for spontaneous release recordings.

Electrophysiological recordings. In sagittal neocortical slices, pyramidal cell recordings were made under visual control (layer 2/3 or 4 with Scientifica Pro 1000) using the patch-clamp technique in the whole cell-configuration with an Axopatch 200B (Molecular Devices). For spontaneous event recordings from slices, 1 μM TTX was added to ACSF before the start of the experiment. Synaptic currents and agonist-evoked responses were acquired with a personal computer using an ITC-16 analog-to-digital converter. To measure postsynaptic currents, we recorded with patch electrodes with a resistance of 5–10 MΩ and used two different intracellular solutions with compositions that allowed us to record spontaneous release at −70 mV. Excitatory events were recorded using a pipette solution with the following composition (in mM): 135 K-gluconate, 4 $MgCl_2$, 10 HEPES, 4 Na-ATP, 0.3 Na-GTP, 10 creatine phosphate at pH 7.2, and 308 mOsm. Inhibitory events were recorded using a similar solution in which potassium gluconate was replaced with potassium chloride. Data were analyzed using Synaptosoft and IgorPro software. As a rule, we started recording no earlier than 10 min after forming whole-cell configuration to provide steady-state value for frequency of postsynaptic currents. Each point on diary plots was obtained by averaging the frequency of events every 27 s for slice preparations and 10 s for culture preparations.

For recordings in transverse brainstem slices, principle neurons were identified under visual control (BX51 WI, Olympus), and recordings were made using the patch-clamp technique in the whole cell-configuration with an EPC 9/2 amplifier (HEKA Elektronik). Currents were filtered at 2.9 kHz using a Bessel filter and sampled at 50 kHz. Series resistance (R_s) was monitored, and only recordings were R_s remained constant (<30% change during a recording) were used. R_s was compensated to 50–70%. Microelectrodes had a resistance of 2.5–4 MΩ and were filled with a solution composed of the following (in mM): 140 K-gluconate, 2 KCl, 5 EGTA, 10 HEPES, 4 Mg-ATP, 0.5 Na-GTP, 5 creatine phosphate, pH 7.2. Na^+ and Cl^- ions had inwardly directed driving forces at −70 mV, making it possible to distinguish them by their polarity (upward for mIPSC and downward for mEPSC). Recordings were obtained at room temperature (24°C), which reduces mEPSC frequencies (Kushmerick et al., 2006). Data were analyzed using IgorPro (RRID:SCR_000325) and Axograph (RRID:SCR_014284).

For recordings in culture, cells were visualized with an Olympus IX70 inverted microscope. Recordings were made in whole-cell voltage-clamp mode in neurons voltage clamped at −70 mV. Voltages were corrected for liquid junction potentials (Hughes et al., 1987). The extracellular solution contained the following (in mM): 150 NaCl, 4 KCl, 10 HEPES, 10 glucose, 1.1 $CaCl_2$, 1.1 $MgCl_2$, pH 7.35, with NaOH unless indicated otherwise. Recordings of mIPSCs were made in the presence of tetrodotoxin (TTX; 1 μM) and CNQX (10 μM) to block Na^+ channels and AMPA receptors, respectively. Spontaneous release from excitatory synapses was resolved by blocking GABA with gabazine (10 μM). The alternative solution used in Figure 6 contained the following (in mM): 125 NaCl, 2.5 KCl, 25 HEPES, 30 glucose, and 2 $MgCl_2$ and $CaCl_2$ at pH 7.35, as used by Ermolyuk et al. (2013). Recordings of mIPSCs were made using a potassium chloride-rich intracellular solution containing the following (in mM): 118 KCl, 1 EGTA, 10 HEPES, 4 $MgCl_2$, 1 $CaCl_2$, 4 NaATP, 0.3 NaGTP, and 14 creatinine phosphate, pH 7.2, with KOH. Electrodes had resistances of 3–7 MΩ. For VACC current recordings, 150 mM TEACl, 1 μM TTX, and 10 μM GABAzine, and CNQX were added to standard extracellular solution, and the patch pipette was filled with a $CsMeSO_3$-rich solution containing the following (in mM): 108 $CsMeSO_3$, 9 EGTA, 10 HEPES, 4 $MgCl_2$, 1 $CaCl_2$, 4 NaATP, 0.3 NaGTP, pH brought to 7.2 using TEAOH. Currents were recorded with a HEKA EPC9/2 amplifier and filtered at 1 kHz using a Bessel filter and sampled at 10 kHz. R_s was monitored, and recordings were discarded if R_s changed significantly during a recording. R_s was compensated to ~70% in recordings of VACC currents.

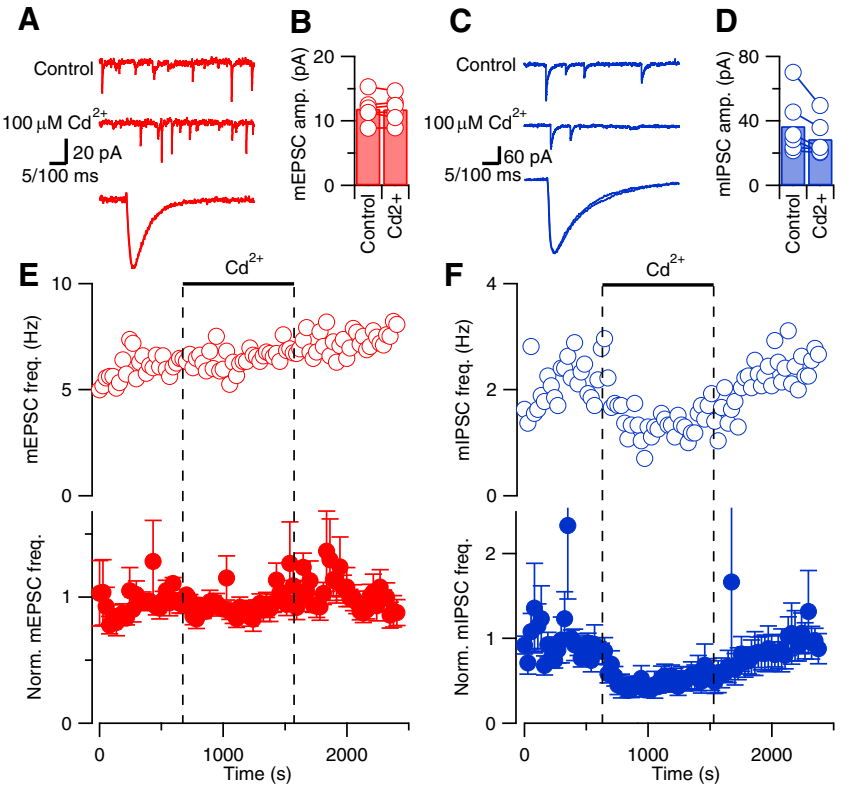

Figure 1. Cd^{2+} reduces spontaneous release of GABA but not glutamate in acute neocortical slices. ***A***, Exemplary current traces showing mEPSCs (red) before (top trace) and during (middle trace) application of 100 μM Cd^{2+}. Calibration: 20 pA, 100 ms. The bottom trace shows superimposed average mEPSCs after normalization for amplitude. Calibration: 5 ms. ***B***, Histogram of average mEPSC amplitude in control conditions and in the last 2 min of Cd^{2+} application. Open circles linked with lines represent average mEPSC amplitudes from individual experiments ($n = 6$). ***C***, Exemplary current traces showing mIPSCs (blue) before (top trace) and during (middle trace) application of 100 μM Cd^{2+}. Calibration: 60 pA, 100 ms. The bottom trace shows superimposed average mIPSCs after normalization for amplitude. Calibration: 5 ms. ***D***, Histogram of average mIPSC amplitude in control conditions and in the last 120 s of Cd^{2+} application ($n = 6$). ***E***, ***F***, Exemplary (open circles) and normalized average (closed circles) diary plots showing the effect of 100 μM Cd^{2+} (bar and dotted lines) on mEPSC (red) and mIPSC (blue) frequency (mean ± SEM) versus time. Average effects measured over the last 5 min of drug application relative to basal frequency (averaged over the 5 min before application) are shown in this figure and diary plots in Figures 4 and 5.

Solution application. In slice recordings, test solutions were applied via slice perfusion apparatus, whereas in recordings from cultured neurons they were gravity fed through a glass capillary (1.2 mm outer diameter) placed ~1 mm from the patch pipette tip. Toxin (Alomone Labs) stock solutions were all made at 1000-fold concentration with distilled water and stored at −20°C. Cytochrome C (0.5 mg/ml) was also added to ω-Conotoxin (MVIIC)-containing solutions to minimize nonselective toxin binding to the apparatus.

Statistical analysis. Data are presented as mean ± SEM with p values, degrees of freedom (df), and sample size (n). Data were normalized to control for biological variability as described for each experiment, but typically using the average from the first 100–200 s of each recording. For each experiment, statistical significance was determined with two-tailed paired t tests (Microsoft Excel). Concentration–effect relationship curves were fit with Hill equations using IgorPro (RRID:SCR_000325).

Results

Differences in spontaneous release at excitatory and inhibitory synapses

VACCs mediate Ca^{2+} influx to trigger action potential-evoked neurotransmitter release. However, at resting membrane potential, the probability of VACC opening is much lower and therefore other mechanisms may regulate spontaneous release. One possibility is that reported differences in sensitivity to VACC blockers at cortical excitatory synapses may arise from differences attributable to cell culture. To remove this possible confounder, we examined spontaneous release of glutamate and GABA in acute neocortical slices. Using whole-cell recordings from neurons in layer 2/3 or 4, voltage clamped at −70 mV, in the presence of 1 μM tetrodotoxin (inhibitory transmission blocked with gabazine), we found that mEPSCs were unaffected by the inorganic, nonselective VACC blocker Cd^{2+} (Fig. 1). The mEPSCs occurred as rapid, transient, down deflections in the current trace that were unaffected in rise time, decay, or amplitude (Fig. 1*A*,*B*) by application of Cd^{2+} (100 μM). Similarly, Cd^{2+} did not affect mIPSC rise time, decay, or amplitude (Fig. 1*C*,*D*; excitatory transmission blocked with CNQX). The frequency of mEPSCs over time was unaffected by the addition of Cd^{2+} in the illustrated recording (Fig. 1*E*, open circles). This was confirmed in the average diary plot of mEPSC frequency versus time (Fig. 1*E*, solid circles), which was unchanged (103 ± 7%, 5 df, $n = 6$, $p = 0.62$), indicating that VACCs were not triggering spontaneous release of glutamate. In contrast, mIPSC frequency clearly and reversibly decreased following Cd^{2+} application in the exemplar and average diary plots (Fig. 1*F*). On average, Cd^{2+} reduced mIPSC frequency to 54 ± 15% of basal frequency, which was significantly different from its actions on the spontaneous release of glutamate ($n = 6$, 5 df, $p = 0.03$). These data indicate stochastic VACC activity did not contribute to spontaneous release at excitatory synapses but regulated a substantial fraction of spontaneous release at inhibitory synapses in neocortical slices.

Differences in potency of Cd^{2+} on spontaneous release and VACC currents

Actions of Cd^{2+} at sites other than VACCs may make it an unreliable tool to investigate VACC coupling and spontaneous release (Ermolyuk et al., 2013). We postulated that if Cd^{2+} modulated mIPSC frequency via its action on VACC alone, then the potency of Cd^{2+} on VACC currents and spontaneous release of GABA should be equivalent. To test this hypothesis, we compared the concentration–effect relationships for Cd^{2+} on VACC currents and mIPSC frequency. Using cultured neocortical neurons, to improve the voltage clamp, we examined the effects of Cd^{2+} on the VACC current elicited by depolarization from −70 to −10 mV every 10 s (Fig. 2*A*). The VACC current amplitude was reversibly decreased by increasing concentrations of Cd^{2+} (Fig. 2*A*–*C*). The plot of normalized inward current at the end of the depolarizing step versus time was used to estimate the block of VACC currents by external Cd^{2+} (Fig. 2*B*). The normalized steady-state inward current was used to measure the concentration–effect relationship for Cd^{2+} and whole-cell VACC currents (Fig. 2*C*; IC_{50} = 1.08 ± 0.03 μM, $n = 12$). In other recordings, spontaneous release of GABA was isolated using TTX and CNQX to block action potentials and glutamatergic transmission, re-

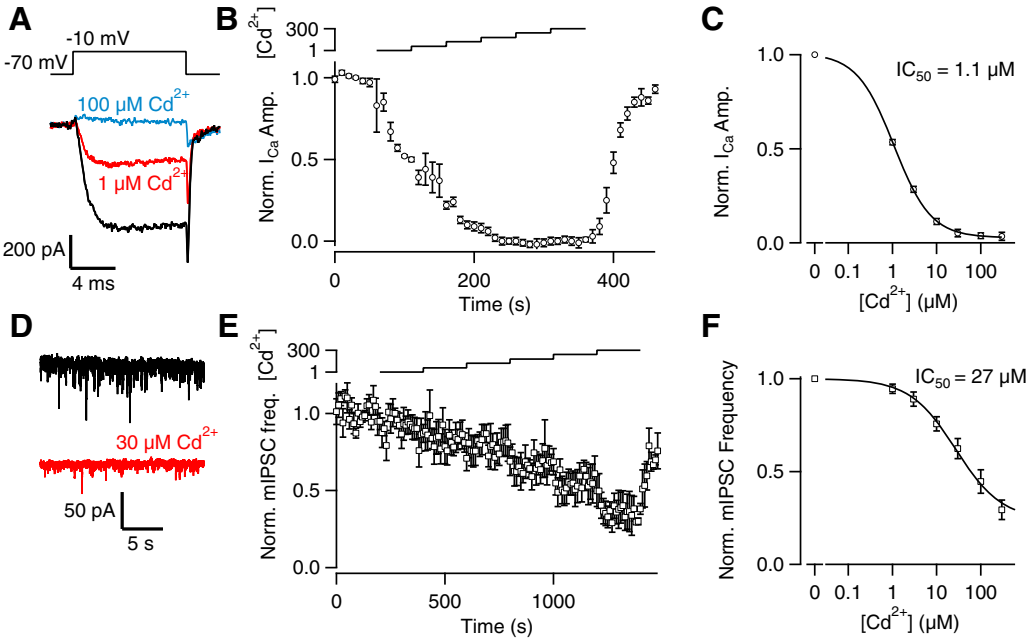

Figure 2. Cd^{2+} apparently blocks VACC currents more potently than it inhibits spontaneous release of GABA. ***A***, VACC currents activated by steps from −70 to −10 mV were substantially reduced by 1 μM (red) or 100 μM Cd^{2+} (blue) ***B***, Average normalized diary plot of VACC current amplitude versus time following application of 0, 1, 3, 10, 30, 100, and 300 μM Cd^{2+} ($n = 12$). The bath contained 1.1 mM Mg^{2+} and 1.1 mM Ca^{2+}, and micromolar [Cd^{2+}] is indicated by the logarithmic scale above the plot. Currents were activated every 10 s, and each cell was normalized according to the average current recorded over the first 60 s. ***C***, Concentration–effect relationship for normalized VACC currents recorded at steady-state [Cd^{2+}] as indicated in ***B***. ***D***, Current traces showing mIPSCs before and during 30 μM Cd^{2+} (red). ***E***, Average normalized diary plot of mIPSC frequency versus time following application of 0, 1, 3, 10, 30, 100, and 300 μM Cd^{2+} ($n = 10$). The bath contained 1.1 mM Mg^{2+} and 1.1 mM Ca^{2+}, and micromolar [Cd^{2+}] is indicated by the logarithmic scale above the plot. Each cell was normalized according to the average mIPSC frequency recorded over the first 200 s. ***F***, Concentration–effect relationship for normalized mIPSC frequency recorded at steady-state [Cd^{2+}] as indicated by the logarithmic scale above the plot in ***E***.

spectively. At −70 mV, mIPSC frequency decreased following the application of 30 μM Cd^{2+} (Fig. 2*D*). The frequency of mIPSCs was measured in contiguous 10 s bins and plotted versus time. Increasing external Cd^{2+} up to 300 μM reversibly reduced mIPSC frequency (Fig. 2*E*), and the plot of normalized steady-state mIPSC frequency versus [Cd^{2+}] revealed a much lower potency (Fig. 2; 27 ± 2.4 μM; $n = 9$) than that observed on VACC currents. This discrepancy was not simply explained by nonlinear coupling between Ca^{2+} entry and the release machinery or differences between terminal and somatic currents because, like VACC currents, action potential-evoked IPSCs were also highly sensitive to Cd^{2+} (IC_{50} = 4.1 ± 0.03 μM, n = 10; data not shown). If the only significant action of Cd^{2+} is to block VACCs, what is the reason for the apparently lower potency of Cd^{2+} on mIPSCs? Can this difference be attribute to actions on VACCs or did it result from effects at other targets?

Cd^{2+} has been shown to have voltage-dependent actions, blocking VACCs less effectively at hyperpolarizing potentials (Chow, 1991). To determine the voltage dependence of Cd^{2+} block of VACC currents under physiological $[Ca^{2+}]_o$ and $[Mg^{2+}]_o$, we elicited VACC currents using a family of voltage steps (from −70 to between −65 and 40 mV for a 10 ms duration) in control conditions (*ICtrl*) and in the presence of Cd^{2+} (1, 100, and 300 μM). [Cd^{2+}], at 100 μM, resulted in saturating VACC current block (data not shown). Currents recorded in 100 μM Cd^{2+} were subtracted from those measured in control conditions and 1 μM Cd^{2+} (*ICd*; Fig. 3*A*,*B*) to isolate the Cd^{2+}-sensitive VACC currents. Application of 1 μM Cd^{2+} reduced current amplitudes, and this block was enhanced at −10 mV compared with −40 mV (Fig. 3*A*). Plotting the currents versus voltage showed that block by 1 μM Cd^{2+} was ~90% at 0 mV (Fig. 3*B*). In some recordings, *ICd* at 0–40 mV increased slightly despite approaching the reversal potential (Fig. 3*B*,*D*). We hypothesized that this effect arose from reduced block by Cd^{2+} at positive potentials or contamination by outward currents through potassium channels despite use of 150 mM Tetraethylammonium (TEA) in bath and cesium in pipette solutions (Adelman and French, 1978; Thévenod and Jones, 1992; Crouzy et al., 2001). Plotting the amplitude of the tail current versus the voltage reduced the impact of any putative contaminating current by reducing the driving voltage for currents through unblocked potassium channels. Tail currents (I_{Tail}) recorded following steps above 0 mV were stable in the presence of 1 μM Cd^{2+} (Fig. 3*C*). The average voltage dependence of block by 1 μM Cd^{2+} was illustrated by replotting *ICdI/ICtrl* versus voltage for both steady-state (Fig. 3*D*; red) and tail currents (blue; $n = 4$). Under these conditions, block by 1 μM Cd^{2+} was 89 ± 5% and 73 ± 6% at ~0 mV for steady-state and tail currents, respectively (Fig. 3*C*; $n = 4$). The lack of decrease of the average tail current with depolarization >0 mV suggests variation of ICd at these voltages was attributable to contaminating currents. We also tested for depolarization-dependent loss of VACC block by low Cd^{2+} by using strong depolarizations that have been shown to rapidly reverse block of VACCs by Cd^{2+} (Thévenod and Jones, 1992). We compared VACC currents activated by a step to −10 mV before (*S1*) and after (*S2*) a depolarization to 130 mV (1–15 ms duration). S1 and S2 were reduced equally by the application of Cd^{2+} (Fig. 3*E*,*F*), indicating the strong depolarizations did not reverse Cd^{2+} block of VACC currents. These results are consistent with there being no rapidly occurring reduction in Cd^{2+} potency at depolarized potentials in these neurons. In addition, the middle pulse activated an outward current that was Cd^{2+} sensitive and thus may account for the apparent variability of I_{8-10} at positive voltages (Fig. 3*D*). At potentials negative to −50 mV, 1 μM Cd^{2+} had no discernible effect

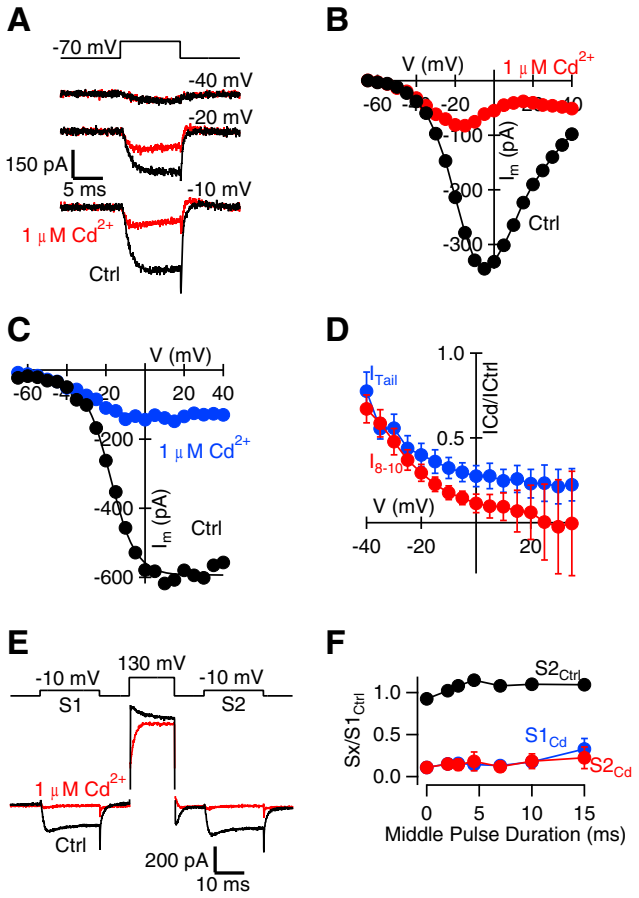

Figure 3. Voltage dependence of Cd^{2+} block of VACC currents. ***A***, Exemplary traces of 100 μM Cd^{2+}-subtracted currents recorded at −40, −20, and −10 mV voltage-step protocols under control conditions (black) and in 1 μM Cd^{2+} (red). Notice the decrease in block at more hyperpolarized steps. ***B***, *I–V* curve for VACC currents measured over the last 2 ms of the 10 ms voltage step (I_{8-10}) from the same experiment in ***A***. ***C***, Plot of the peak amplitude of the tail currents from the same experiment versus the voltage step from the same experiment in ***A***. Tail currents recorded in control conditions are indicated in black, and those recorded in the presence of 1 μM Cd^{2+} are indicated in blue. Tail current amplitude is measured as the minimum occurring within 200 μs after the voltage step. ***D***, Plot of VACC current amplitude (red, I_{8-10}) and tail current amplitude (blue, I_{Tail}) in 1 μM Cd^{2+} divided by that measured in control conditions and plotted against membrane potential ($n = 4$). Note the reduced block by Cd^{2+} at more hyperpolarized potentials and the increase in variability of the steady-state current at positive potentials. ***E***, Exemplary traces of currents recorded in control conditions (black) and in 1 μM Cd^{2+} (red) with prepulse and postpulse currents (S1 and S2, respectively) recorded at −10 mV, where the current amplitude was maximal and the middle pulse was 130 mV. The middle pulse was increased in duration from 0 to 15 ms. Note the presence of the Cd^{2+}-sensitive outward current resulting from the middle pulse. ***F***, Plot of the ratio of the peak amplitude of the current measured (S_x) to the peak amplitude of the current measured for S1 under control conditions versus the duration of the middle pulse ($n = 3$). S_x described S2 under control conditions (black) or in the presence of 1 μM Cd^{2+} at either S1 (blue) or S2 (red). Error bars indicate SEM.

on VACC tail currents. Since mIPSCs were recorded when the presynaptic membrane potential was hyperpolarized (−70 to −80 mV), these results explain why higher concentrations of Cd^{2+} were required to inhibit mIPSCs (Fig. 2*F*) than the VACC currents activated by steps to −10 mV or stimulus-evoked IPSCs, and obviates the need to propose off-target effects of Cd^{2+} to explain its action on mIPSCs (Ermolyuk et al., 2013).

Specific blockers of VACCs on spontaneous release

To further test the action of VACC activity on spontaneous release, we used a structurally different type of VACC blocker, MVIIC, which is a peptide toxin specific for block of N- and P/Q-type VACCs. N-, P/Q-, and R-type VACCs are expressed in neocortical nerve terminals and have been shown to contribute to spontaneous and evoked release at these synapses (Cao and Tsien, 2005; Bucurenciu et al., 2010). Application of a saturating concentration of MVIIC (5 μM) had no effect on mEPSC or mIPSC rise time, decay phase, or amplitude (Fig. 4*A–D*). However, MVIIC reduced mIPSC frequency to 47 ± 9% of basal level ($p = 0.002$, 5 df, $n = 6$) while having no effect on mEPSC frequency (100 ± 6% of baseline, $n = 5$), as illustrated by the exemplar and average diary plots (Fig. 4*E*,*F*). Similar to the experiments using Cd^{2+} to block VACC currents (Fig. 1), these findings confirmed that VACCs strongly regulate spontaneous synaptic transmission at inhibitory synapses but not at excitatory synapses. Moreover, the degree of reduction of mIPSC frequency by MVIIC seen here is similar to that described previously using saturating doses of selective VACC blockers in cultured neurons (Williams et al., 2012).

Spontaneous glutamate release is not triggered by VACCs at the calyx of Held synapse

How wide-ranging is the difference in regulation of spontaneous release from excitatory and inhibitory synapses? We asked whether excitatory and inhibitory synapses in other areas of the CNS were regulated similarly. To answer this question, we recorded from principal cells of the MNTB in acute mouse auditory brainstem slices (Fig. 5). One advantage of this preparation is that principal cells usually receive one large glutamatergic calyx-type synapse on their soma and multiple small bouton-type inhibitory synapses that release glycine or GABA (von Gersdorff and Borst, 2002). Thus, in voltage-clamp mode, we acquired and resolved mEPSCs and mIPSCs simultaneously from the same postsynaptic cell by using bath and pipette solutions that widely separated the reversal potentials for excitatory and inhibitory transmissions (see Materials and Methods; Fig. 5*A*,*B*). At this developmental stage (postnatal day 10 to 12), mIPSCs reflect spontaneous release of glycine or GABA (Awatramani et al., 2005). Using a bicarbonate-based external solution with 1.5 mM Ca^{2+}, the application of Cd^{2+} (50 μM) blocked EPSCs evoked by afferent fiber stimulation (data not shown; but see Taschenberger and von Gersdorff, 2000; Mintz et al., 1995), but had no effect on the size or time course of the mEPSCs or mIPSCs (Fig. 5*A*,*B*). However, Cd^{2+} reduced mIPSC frequency by 73 ± 12% ($p < 0.0001$ 4 df, $n = 5$), whereas it did not affect mEPSC frequency significantly (Fig. 5*C*,*D*; 123 ± 45% of basal, $p = 0.247$, 4 df, $n = 5$). Note also that the effect of Cd^{2+} on the mIPSC frequency was fully reversible (see also Fig. 1*F*), again suggesting that it did not have major off-target effects. These data are consistent with our observations in acute neocortical slices and cultured neocortical neurons. They confirm and extend our findings that presynaptic VACCs regulate spontaneous release at inhibitory but not at excitatory CNS synapses.

Spontaneous release at excitatory terminals and neuronal excitability

Previous reports suggesting that VACCs regulate spontaneous release at excitatory synapses have used an external solution with higher glucose, HEPES, Mg^{2+}, and Ca^{2+} concentrations and lower K^+ concentration (Ermolyuk et al., 2013). We thus tested whether this alternative solution increased the sensitivity of spontaneous release of glutamate to VACC blockers (Fig. 6; Vyleta and Smith, 2011; Ermolyuk et al., 2013). We found that 100 μM Cd^{2+} did not elicit a decrease in mEPSC frequency in

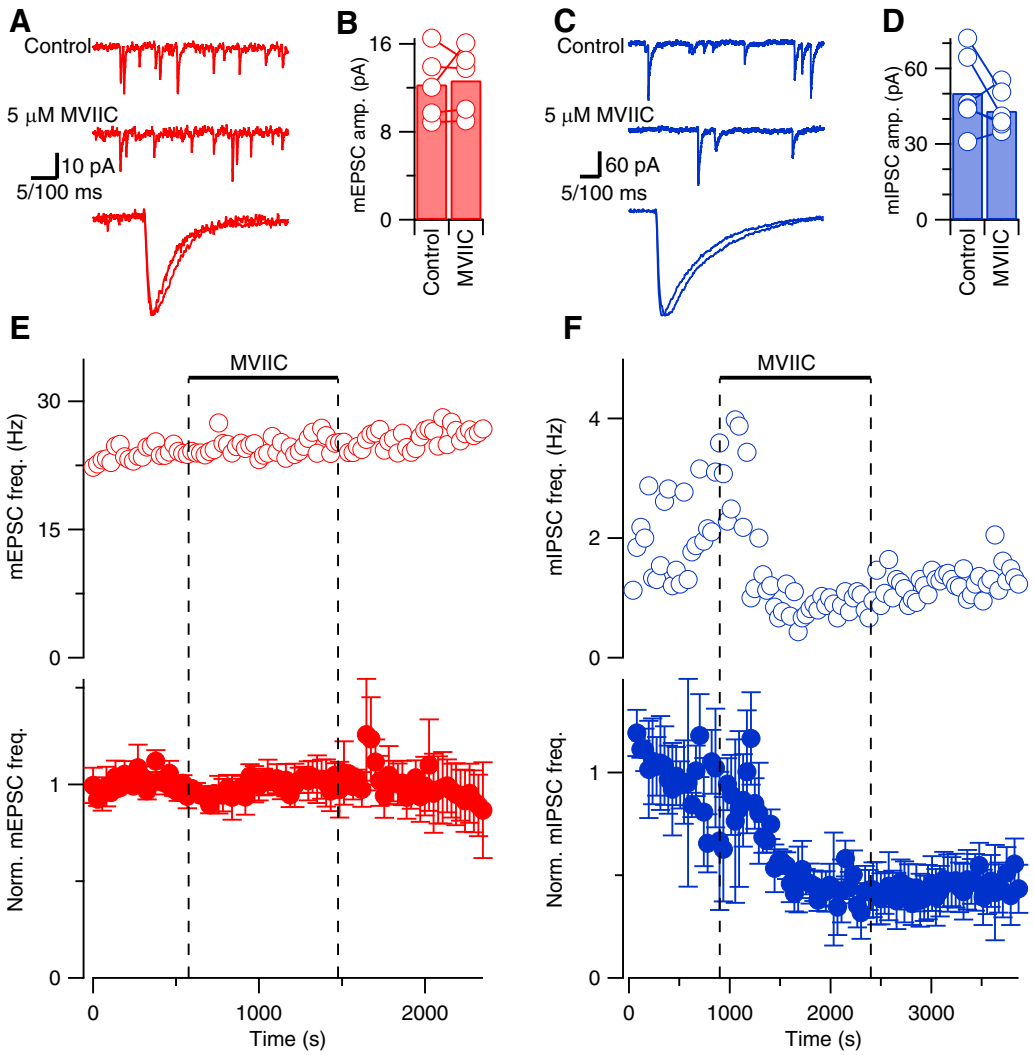

Figure 4. MVIIC reduces spontaneous release of GABA but not glutamate in acute neocortical slices. ***A***, Exemplary current traces showing mEPSCs (red) before (top trace) and during (middle trace) application of 5 μM MVIIC. Calibration: 100 ms. The bottom trace shows superimposed average mEPSCs after normalization for amplitude. Calibration: 5 ms. ***B***, Histogram of average mEPSC amplitudes in control conditions and in the last 120 s of MVIIC application. Open circles linked with lines represent average mEPSC amplitudes from individual experiments ($n = 5$). ***C***, Exemplary current traces showing mIPSCs (blue) before (top trace) and during (middle trace) application of 5 μM MVIIC. Calibration: 100 ms. The bottom trace shows superimposed average mIPSCs after normalization for amplitude. Calibration: 5 ms. ***D***, Histogram of average mIPSC amplitudes in control conditions and in the last 120 s of MVIIC application ($n = 6$). ***E***, ***F***, Exemplary (open circles) and normalized average (closed circles) diary plots showing the effect of 5 μM MVIIC (bar and dotted lines) on mEPSC (red) and mIPSC (blue) frequency (mean ± SEM) versus time.

control Tyrode (Fig. 6*B*; 1.68 ± 0.3 Hz) or alternative Tyrode solution (Fig. 6*B*; 1.54 ± 0.2 Hz in Cd^{2+}). Cd^{2+} slightly increased the mEPSC frequency, as reported previously (Vyleta and Smith, 2011). This facilitation of spontaneous glutamate release may be due to activation of the Ca^{2+} sensing receptor (CaSR) by Cd^{2+}, which has been suggested to be an agonist along with other divalent cations including Mg^{2+} and Gd^{2+} (Vyleta and Smith, 2011; Smith et al., 2012). Note, however, that we did not see a significant increase of mEPSC frequency at the calyx of Held synapses (Fig. 5*C*), so this Cd^{2+} effect may be synapse dependent. We did not examine whether spontaneous release of glutamate became VACC dependent after more prolonged exposure to the alternative solution.

Discussion

We previously determined that VACCs trigger spontaneous release at inhibitory but not excitatory central synapses in cultured neocortical neurons (Vyleta and Smith, 2011; Williams et al., 2012). More recently it was proposed that VACCs trigger spontaneous release at excitatory synapses in cultured hippocampal neurons and acute slices from the MNTB, and that the use of Cd^{2+} as a VACC blocker may have confounded our experiments (Ermolyuk et al., 2013; Dai et al., 2015). Here we describe experiments that confirm and extend our original findings that VACCs do not trigger spontaneous release at excitatory synapses, but play a major role in spontaneous release at inhibitory synapses. First, we establish that the distinct actions of VACC blockade on excitatory and inhibitory spontaneous release are apparent when VACCs are blocked using Cd^{2+} and by the specific N- and P/Q-type VACC blocker, MVIIC, obviating concern for off-target actions of Cd^{2+}. Second, these distinct actions of VACC inhibition occur in both acute brain slices from the neocortex and brainstem and cultured neocortical neurons, consistent with this effect extending to other areas of the CNS. Third, we find that Cd^{2+} block is voltage dependent, and this likely contributes to discrepancies in VACC regulation of spontaneous and evoked release. Thus, through extensive study, we confirm that VACCs play a substan-

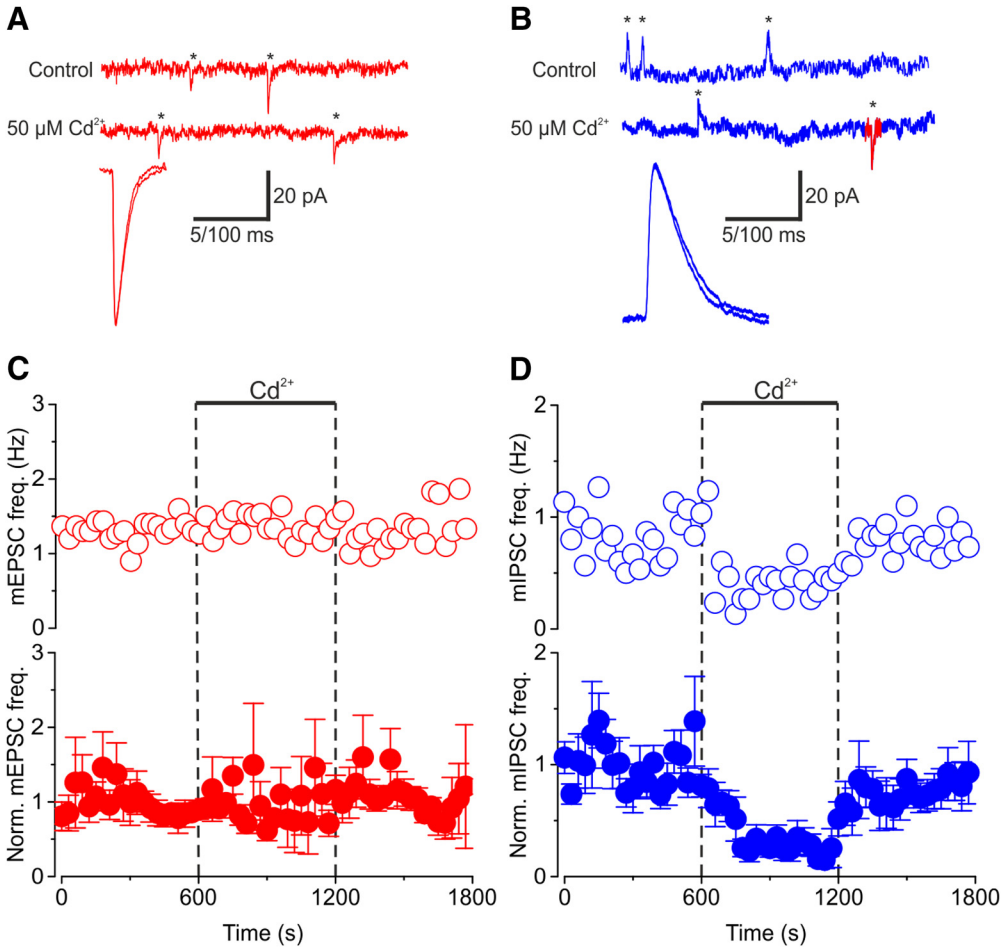

Figure 5. Cd^{2+} reduces spontaneous release of GABA and glycine but not glutamate in acute auditory brainstem slices. ***A***, Exemplary current traces showing mEPSCs (red) before (top trace) and during (middle trace) application of 50 μM Cd^{2+}. Asterisks denote individual release events. The bottom trace shows superimposed average mEPSCs after normalization for amplitude. ***B***, Exemplary current traces showing mIPSCs (blue) before (top trace) and during (middle trace) application of 50 μM Cd^{2+}. Note simultaneously recorded mEPSCs denoted in red. The bottom trace shows superimposed average mIPSCs after normalization for amplitude. ***C***, ***D***, Exemplary (open circles) and normalized average (closed circles) diary plots showing the effect of 50 μM Cd^{2+} (bar and dotted lines) on mEPSC (red) and mIPSC (blue) frequency (mean ± SEM) versus time. Calibrations: ***A***, ***B***, Top, middle traces, 20 pA, 100 ms; bottom traces, 5 ms.

tial role in regulating spontaneous release at inhibitory nerve terminals but not excitatory nerve terminals, where other mechanisms likely contribute to the Ca^{2+} dependence of release.

Differences between release at excitatory and inhibitory terminals

Our findings that block of presynaptic VACCs reduces spontaneous release at inhibitory but not excitatory synapses indicate that there may be important differences in regulation of spontaneous release of GABA and glutamate by VACCs. Other substantial differences in regulatory mechanisms between excitatory and inhibitory terminals have been identified. For example, agonists for endocannabinoid receptors suppress inhibitory activity-evoked release onto Purkinje cells in cerebellum, but reduce spontaneous release only at inhibitory and not excitatory synapses (Yamasaki et al., 2006). Furthermore, inhibitory terminals in hippocampus were found to be more Ca^{2+} sensitive than excitatory terminals synapsing on the same cell because of a deficiency in the SNARE protein SNAP-25 (Verderio et al., 2004). Additionally, differences in membrane ultrastructure that reflect the composition and organization of synaptic proteins have been observed between excitatory and inhibitory contacts (Landis and Reese, 1974).

More studies are necessary to determine the mechanisms underlying this heterogeneity, which include the following potential differences between excitatory and inhibitory synapses in resting membrane potential, type or number of VACCs, size of the Ca^{2+} domain for release, tightness of coupling between VACCs and vesicles, concentrations and potency of intracellular Ca^{2+} buffers, or the proteins that comprise the release machinery. Models indicate that a 10 mV hyperpolarization in membrane potential would substantially reduce the stochastic activity of VACCs at the nerve terminal and almost eliminate VACC-dependent spontaneous release (Ermolyuk et al., 2013), but technical difficulties have prevented direct testing of this hypothesis to date. Intersynaptic variation of synaptic protein isoforms is well recognized (Geppert et al., 1994; Sun et al., 2007) and is one potential mechanism to explain why VACCs trigger spontaneous release at inhibitory but not excitatory synapses. Since VACCs trigger evoked release at both types of synapses, this explanation would also necessitate that different synaptic proteins mediate evoked and spontaneous release (Crawford and Kavalali, 2015) or that the same synaptic protein mediate evoked and spontaneous release via different molecular states (Dai et al., 2015). In addition, there would have to be wide variation in calcium sensitivities for different isoforms of synaptic protein to account for the difference between excitatory and inhibitory synapses. Further complexity is suggested by findings at ribbons synapses, which operate via graded membrane potential changes, where the rate of flicker

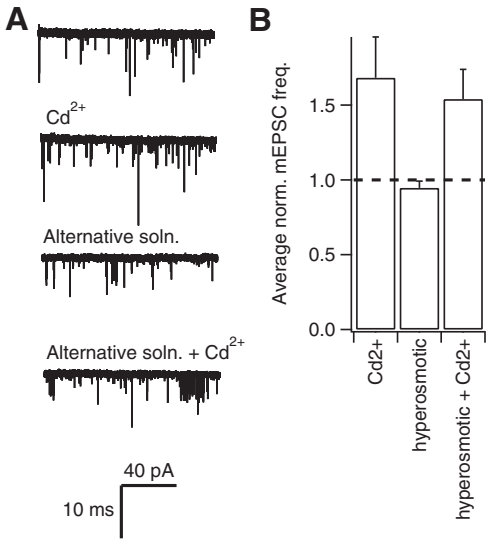

Figure 6. An alternative external solution does not affect resistance of mEPSC frequency to Cd^{2+}. ***A***, Exemplary current traces show mEPSCs recorded before and after the application of 100 μM Cd^{2+} in control conditions and in an alternative extracellular solution that contained lower Na^{+} concentration and higher glucose and HEPES concentrations. ***B***, Histogram showing the average effect of Cd^{2+} in control and alternative solutions ($n = 6$). Average mEPSC frequency was measured over the 200 s before Cd^{2+} application and used to normalize each recording. The average mEPSC frequencies represent steady-state data collected over a 100 s epoch once the test solutions had been applied for 100 s.

from the closed to the open state of single VACCs may regulate the frequency of mEPSCs (Graydon et al., 2011; Kim et al., 2013). In fact, recent studies demonstrate both Ca^{2+}-dependent and Ca^{2+}-independent mEPSC frequency at retinal ribbon synapses (Cork et al., 2016).

Variation in VACC regulation of neurotransmitter release

A majority of investigators have reported that block of VACCs does not reduce spontaneous release of glutamate at central excitatory synapses. In cultured hippocampal neurons, Cd^{2+} did not affect mEPSC frequency (Abenavoli et al., 2002; Yamasaki et al., 2006). In cultured neurons from neocortex, VACC block with Cd^{2+} or MVIIC did not reduce mEPSC frequency (Vyleta and Smith, 2011). In hippocampal slices, spontaneous release of glutamate was also independent of VACC activity (Eggermann et al., 2011). This contrasts with observations made at inhibitory synapses, where there have been numerous reports that VACCs regulate spontaneous release of GABA. This finding has been confirmed in cultured neocortical neurons (Yamasaki et al., 2006; Williams et al., 2012) and acute hippocampal slices (Goswami et al., 2012). The resistance of spontaneous release of glutamate to VACC blockers we report here is also consistent with previous observations that buffering intracellular $[Ca^{2+}]$ ($[Ca^{2+}]_i$) with BAPTA did not affect mEPSC frequency at these synapses (Abenavoli et al., 2002; Vyleta and Smith, 2011). This contrasts with observations where spontaneous release at excitatory synapses was sensitive to VACC blockers and also sensitive to BAPTA (Ermolyuk et al., 2013).

How do we explain the reported sensitivity of spontaneous release of glutamate to VACC blockers at hippocampal, neocortical, and brainstem synapses (Xu et al., 2009; Ermolyuk et al., 2013; Dai et al., 2015)? One explanation is that Cd^{2+} may be acting to impair synaptic transmission via off-target mechanisms (Ermolyuk et al., 2013). This idea arose because Cd^{2+} is known to permeate VACCs and directly increase Fluo-4 fluorescence (Hinkle et al., 1992; Spence and Johnson, 2010; Lopin et al., 2012). We hypothesized that in the absence of off-target actions, Cd^{2+} would inhibit VACC currents and spontaneous release similarly. As we observed no effect of Cd^{2+} on spontaneous release of glutamate, we investigated its action at inhibitory synapses. We found Cd^{2+} was more potent on VACC currents than on spontaneous release (Fig. 2), potentially refuting our hypothesis. However, Cd^{2+} exhibits a voltage-dependent block, with Cd^{2+} being less effective at negative potentials in squid axons (Chow, 1991). Since we studied the effects of Cd^{2+} on VACC currents and spontaneous release at very different voltages (−10 and ~−75 mV respectively), we tested whether Cd^{2+} caused voltage-dependent block at the relevant concentration range (1–300 μM) with 1.1 mM Ca^{2+} and Mg^{2+} in the external solution. While ≥100 μM Cd^{2+} fully blocked VACC currents, 1 μM Cd^{2+} blocked a large fraction of the VACC current at −10 mV but had a smaller effect on VACC currents at the voltage range relevant to spontaneous release. Only by increasing the $[Cd^{2+}]$, and thus overcoming the voltage-dependent block, did we observe an effect on spontaneous release (Fig. 2). Likewise, 3 μM Cd^{2+} blocks 60% of the evoked EPSCs at cerebellar granule cell to Purkinje cell synapses, indicating Cd^{2+} is more effective when the nerve terminal is depolarized by stimulation (Mintz et al., 1995). Thus voltage-dependent block explains the discrepancy in potency of Cd^{2+} on VACC currents and mIPSC frequency. Independent support for this hypothesis comes from our observations that the selective N- and P/Q-type VACC blocker MVIIC reduced mIPSC frequency but did not affect spontaneous release of glutamate in neocortical neurons in slice (Fig. 4). Differences in external solution could alter resting membrane potential and thereby alter the response of excitatory terminals to VACC blockers. It has been demonstrated that depolarizing the resting membrane potential increases spontaneous release, and hyperpolarizing has the opposite effect (Angleson and Betz, 2001; Li et al., 2009; Graydon et al., 2011; Williams et al., 2012). In addition, a high concentration of extracellular HEPES causes intracellular alkalinization, which can affect vesicular endocytosis (Zhang et al., 2010), as well as synaptic cleft and vesicle acidification (Cho and von Gersdorff, 2014). Additionally, elevated glucose has been demonstrated to lead to oxidative damage and apoptosis in neurons (Vincent et al., 2005). As an alternative external solution had no effect on the response of excitatory terminals to Cd^{2+}, the cause of the difference remains uncertain. It is possible that a relatively depolarized resting membrane potential and/or small differences in animal age could account for the sensitivity of spontaneous excitatory transmission to VACC blockers (Ermolyuk et al., 2013; Dai et al., 2015). However, the mechanism to account for this difference has not been identified, and the consistency between our new acute slice and culture data supports our previous conclusions.

Alternatives to VACCs for Ca^{2+} regulation

Increases in $[Ca^{2+}]_i$ independent of VACCs has been shown to increase spontaneous release at excitatory and inhibitory synapses (Llano et al., 2000; Yamasaki et al., 2006; Vyleta and Smith, 2008). In addition, the lack of effect of strong buffering of $[Ca^{2+}]_i$ on steady-state mEPSC frequency has pointed to a potential role for other pathways independent of $[Ca^{2+}]_i$ (Vyleta and Smith, 2011). Consistent with this hypothesis, mEPSC frequency was proportional to external $[Mg^{2+}]$ ($[Mg^{2+}]_o$), which might have been expected to reduce spontaneous release at excitatory and inhibitory synapses via VACC block (Vyleta and Smith, 2011). The Ca^{2+} sensing receptor, which is localized to the presynaptic membrane (Ruat et al., 1995; Chen et al., 2010), may trigger

spontaneous vesicle fusion via a mechanism that is independent of $[Ca^{2+}]_i$ but sensitive to $[Ca^{2+}]_o$ and $[Mg^{2+}]_o$. CaSR agonists stimulate spontaneous glutamate and GABA release (Vyleta and Smith, 2011; Smith et al., 2012). Spontaneous release of glutamate may also be triggered by long lasting increases in basal $[Ca^{2+}]_i$, since Ca^{2+} chelators act by attenuating transient changes (Pethig et al., 1989).

Conclusions

It is well established that activity-dependent neurotransmitter release is highly dependent on $[Ca^{2+}]_o$. While spontaneous release of GABA has much weaker $[Ca^{2+}]_o$ dependence, here we show that VACCs are still the main Ca^{2+} source for release. This finding contrasts with the VACC independence of spontaneous release at excitatory synapses and has been confirmed by a majority of studies from central synapses in culture and in slices. Understanding the mechanisms by which Ca^{2+} influences the different modes of neurotransmitter release will improve our knowledge of synaptic function in general and of disrupted transmission in disease states.

References

Abenavoli A, Forti L, Bossi M, Bergamaschi A, Villa A, Malgaroli A (2002) Multimodal quantal release at individual hippocampal synapses: evidence for no lateral inhibition. J Neurosci 22:6336–6346. Medline

Adelman WJ Jr, French RJ (1978) Blocking of the squid axon potassium channel by external caesium ions. J Physiol 276:13–25. CrossRef Medline

Angleson JK, Betz WJ (2001) Intraterminal Ca2+ and spontaneous transmitter release at the frog neuromuscular junction. J Neurophysiol 85:287–294. Medline

Autry AE, Adachi M, Nosyreva E, Na ES, Los MF, Cheng PF, Kavalali ET, Monteggia LM (2011) NMDA receptor blockade at rest triggers rapid behavioural antidepressant responses. Nature 475:91–95. CrossRef Medline

Awatramani GB, Turecek R, Trussell LO (2005) Staggered development of GABAergic and glycinergic transmission in the MNTB. J Neurophysiol 93:819–828. Medline

Borst JG, Sakmann B (1996) Calcium influx and transmitter release in a fast CNS synapse. Nature 383:431–434. CrossRef Medline

Bucurenciu I, Bischofberger J, Jonas P (2010) A small number of open Ca^{2+} channels trigger transmitter release at a central GABAergic synapse. Nat Neurosci 13:19–21. CrossRef Medline

Cao YQ, Tsien RW (2005) Effects of familial hemiplegic migraine type 1 mutations on neuronal P/Q-type Ca^{2+} channel activity and inhibitory synaptic transmission. Proc Natl Acad Sci U S A 102:2590–2595. CrossRef Medline

Carter AG, Regehr WG (2002) Quantal events shape cerebellar interneuron firing. Nat Neurosci 5:1309–1318. CrossRef Medline

Chen W, Bergsman JB, Wang X, Gilkey G, Pierpoint CR, Daniel EA, Awumey EM, Dauban P, Dodd RH, Ruat M, Smith SM (2010) Presynaptic external calcium signaling involves the calcium-sensing receptor in neocortical nerve terminals. PLoS One 5:e8563. CrossRef Medline

Cho S, von Gersdorff H (2014) Proton-mediated block of Ca^{2+} channels during multivesicular release regulates short-term plasticity at an auditory hair cell synapse. J Neurosci 34:15877–15887. CrossRef Medline

Chow RH (1991) Cadmium block of squid calcium currents. Macroscopic data and a kinetic model. J Gen Physiol 98:751–770. CrossRef Medline

Cohen I, Miles R (2000) Contributions of intrinsic and synaptic activities to the generation of neuronal discharges in *in vitro* hippocampus. J Physiol 524:485–502. CrossRef Medline

Cork KM, Van Hook MJ, Thoreson WB (2016) Mechanisms, pools, and sites of spontaneous vesicle release at synapses of the rod and cone photoreceptors. Eur J Neurosci 44:2015–2027. CrossRef

Crawford DC, Kavalali ET (2015) Molecular underpinnings of synaptic vesicle pool heterogeneity. Traffic 16:338–364. CrossRef Medline

Crouzy S, Bernèche S, Roux B (2001) Extracellular blockade of K^+ channels by TEA: results from molecular dynamics simulations of the KcsA channel. J Gen Physiol 118:207–218. CrossRef Medline

Dai J, Chen P, Tian H, Sun J (2015) Spontaneous vesicle release is not tightly coupled to voltage-gated calcium channel-mediated Ca^{2+} influx and is triggered by a Ca^{2+} sensor other than synaptotagmin-2 at the juvenile mice calyx of held synapses. J Neurosci 35:9632–9637. CrossRef Medline

Eggermann E, Bucurenciu I, Goswami SP, Jonas P (2011) Nanodomain coupling between Ca^{2+} channels and sensors of exocytosis at fast mammalian synapses. Nat Rev Neurosci 13:7–21. CrossRef Medline

Ermolyuk YS, Alder FG, Surges R, Pavlov IY, Timofeeva Y, Kullmann DM, Volynski KE (2013) Differential triggering of spontaneous glutamate release by P/Q-, N- and R-type Ca^{2+} channels. Nat Neurosci 16:1754–1763. CrossRef Medline

Forsythe ID (1994) Direct patch recording from identified presynaptic terminals mediating glutamatergic EPSCs in the rat CNS, *in vitro*. J Physiol 479:381–387. CrossRef Medline

Geppert M, Goda Y, Hammer RE, Li C, Rosahl TW, Stevens CF, Südhof TC (1994) Synaptotagmin I: a major Ca2+ sensor for transmitter release at a central synapse. Cell 79:717–727. CrossRef Medline

Goswami SP, Bucurenciu I, Jonas P (2012) Miniature IPSCs in hippocampal granule cells are triggered by voltage-gated Ca^{2+} channels via microdomain coupling. J Neurosci 32:14294–14304. CrossRef Medline

Graydon CW, Cho S, Li GL, Kachar B, von Gersdorff H (2011) Sharp Ca^{2+} nanodomains beneath the ribbon promote highly synchronous multivesicular release at hair cell synapses. J Neurosci 31:16637–16650. CrossRef Medline

Hinkle PM, Shanshala ED 2nd, Nelson EJ (1992) Measurement of intracellular cadmium with fluorescent dyes. Further evidence for the role of calcium channels in cadmium uptake. J Biol Chem 267:25553–25559. Medline

Hughes D, McBurney RN, Smith SM, Zorec R (1987) Cesium ions activate chloride channels in rat cultured spinal cord neurones. J Physiol 392:231–251. CrossRef Medline

Jensen K, Jensen MS, Lambert JD (1999) Post-tetanic potentiation of GABAergic IPSCs in cultured rat hippocampal neurones. J Physiol 519:71–84. CrossRef Medline

Kavalali ET, Chung C, Khvotchev M, Leitz J, Nosyreva E, Raingo J, Ramirez DM (2011) Spontaneous neurotransmission: an independent pathway for neuronal signaling? Physiology 26:45–53. CrossRef Medline

Kim MH, Li GL, von Gersdorff H (2013) Single Ca^{2+} channels and exocytosis at sensory synapses. J Physiol 591:3167–3178. CrossRef Medline

Kombian SB, Hirasawa M, Mouginot D, Chen X, Pittman QJ (2000) Short-term potentiation of miniature excitatory synaptic currents causes excitation of supraoptic neurons. J Neurophysiol 83:2542–2553. Medline

Kushmerick C, Renden R, von Gersdorff H (2006) Physiological temperatures reduce the rate of vesicle pool depletion and short-term depression via an acceleration of vesicle recruitment. J Neurosci 26:1366–1377. CrossRef Medline

Landis DM, Reese TS (1974) Differences in membrane structure between excitatory and inhibitory synapses in the cerebellar cortex. J Comp Neurol 155:93–125. CrossRef Medline

Li GL, Keen E, Andor-Ardó D, Hudspeth AJ, von Gersdorff H (2009) The unitary event underlying multiquantal EPSCs at a hair cell's ribbon synapse. J Neurosci 29:7558–7568. CrossRef Medline

Llano I, González J, Caputo C, Lai FA, Blayney LM, Tan YP, Marty A (2000) Presynaptic calcium stores underlie large-amplitude miniature IPSCs and spontaneous calcium transients. Nat Neurosci 3:1256–1265. CrossRef Medline

Llinás RR, Sugimori M, Cherksey B (1989) Voltage-dependent calcium conductances in mammalian neurons. The P channel. Ann N Y Acad Sci 560:103–111. CrossRef

Lopin KV, Thévenod F, Page JC, Jones SW (2012) Cd^{2+} block and permeation of $Ca_V3.1$ (α1G) T-type calcium channels: candidate mechanism for Cd^{2+} influx. Mol Pharmacol 82:1183–1193. CrossRef Medline

Matthews G, Wickelgren WO (1977) On the effect of calcium on the frequency of miniature end-plate potentials at the frog neuromuscular junction. J Physiol 266:91–101. CrossRef Medline

McKinney RA, Capogna M, Dürr R, Gähwiler BH, Thompson SM (1999) Miniature synaptic events maintain dendritic spines via AMPA receptor activation. Nat Neurosci 2:44–49. CrossRef Medline

Mintz IM, Sabatini BL, Regehr WG (1995) Calcium control of transmitter release at a cerebellar synapse. Neuron 15:675–688. CrossRef Medline

Pethig R, Kuhn M, Payne R, Adler E, Chen TH, Jaffe LF (1989) On the dissociation constants of BAPTA-type calcium buffers. Cell Calcium 10:491–498. CrossRef Medline

Phillips CG, Harnett MT, Chen W, Smith SM (2008) Calcium-sensing receptor activation depresses synaptic transmission. J Neurosci 28:12062–12070. CrossRef Medline

Ruat M, Molliver ME, Snowman AM, Snyder SH (1995) Calcium sensing receptor: molecular cloning in rat and localization to nerve terminals. Proc Natl Acad Sci U S A 92:3161–3165. CrossRef Medline

Smith SM, Chen W, Vyleta NP, Williams C, Lee CH, Phillips C, Andresen MC (2012) Calcium regulation of spontaneous and asynchronous neurotransmitter release. Cell Calcium 52:226–233. CrossRef Medline

Spence MT, Johnson ID (2010) The molecular probes handbook: a guide to fluorescent probes and labeling technologies (11th Ed.). Waltham, MA: Life Technologies Corporation.

Sun J, Pang ZP, Qin D, Fahim AT, Adachi R, Südhof TC (2007) A dual-Ca2 -sensor model for neurotransmitter release in a central synapse. Nature 450:676–682. CrossRef Medline

Sutton MA, Schuman EM (2006) Dendritic protein synthesis, synaptic plasticity, and memory. Cell 127:49–58. CrossRef Medline

Taschenberger H, von Gersdorff H (2000) Fine-tuning an auditory synapse for speed and fidelity: developmental changes in presynaptic waveform, EPSC kinetics, and synaptic plasticity. J Neurosci 20:9162–9173. Medline

Thévenod F, Jones SW (1992) Cadmium block of calcium current in frog sympathetic neurons. Biophys J 63:162–168. CrossRef Medline

Verderio C, Pozzi D, Pravettoni E, Inverardi F, Schenk U, Coco S, Proux-Gillardeaux V, Galli T, Rossetto O, Frassoni C, Matteoli M (2004) SNAP-25 modulation of calcium dynamics underlies differences in GABAergic and glutamatergic responsiveness to depolarization. Neuron 41:599–610. CrossRef Medline

Verhage M, Maia AS, Plomp JJ, Brussaard AB, Heeroma JH, Vermeer H, Toonen RF, Hammer RE, van den Berg TK, Missler M, Geuze HJ, Südhof TC (2000) Synaptic assembly of the brain in the absence of neurotransmitter secretion. Science 287:864–869. CrossRef Medline

Vincent AM, Stevens MJ, Backus C, McLean LL, Feldman EL (2005) Cell culture modeling to test therapies against hyperglycemia-mediated oxidative stress and injury. Antioxid Redox Signal 7:1494–1506. CrossRef Medline

von Gersdorff H, Borst JG (2002) Short-term plasticity at the calyx of Held. Nat Neurosci 3:53–64. CrossRef

Vyleta NP, Smith SM (2008) Fast inhibition of glutamate-activated currents by caffeine. PLoS One 3:e3155. CrossRef Medline

Vyleta NP, Smith SM (2011) Spontaneous glutamate release is independent of calcium influx and tonically activated by the calcium-sensing receptor. J Neurosci 31:4593–4606. CrossRef Medline

Wheeler DB, Randall A, Tsien RW (1994) Roles of N-type and Q-type Ca2+ channels in supporting hippocampal synaptic transmission. Science 264:107–111. CrossRef Medline

Williams C, Chen W, Lee CH, Yaeger D, Vyleta NP, Smith SM (2012) Coactivation of multiple tightly coupled calcium channels triggers spontaneous release of GABA. Nat Neurosci 15:1195–1197. CrossRef Medline

Xu J, Jun X, Pang ZP, Shin OH, Südhof TC (2009) Synaptotagmin-1 functions as a Ca^{2+} sensor for spontaneous release. Nat Neurosci 12:759–766. CrossRef Medline

Yamasaki M, Hashimoto K, Kano M (2006) Miniature synaptic events elicited by presynaptic Ca^{2+} rise are selectively suppressed by cannabinoid receptor activation in cerebellar Purkinje cells. J Neurosci 26:86–95. CrossRef Medline

Zhang Z, Nguyen KT, Barrett EF, David G (2010) Vesicular ATPase inserted into the plasma membrane of motor terminals by exocytosis alkalinizes cytosolic pH and facilitates endocytosis. Neuron 68:1097–1108. CrossRef Medline